CONTINUOUS SUCCINIC ACID PRODUCTION BY *ACTINOBACILLUS SUCCINOGENES* IN A BIOFILM REACTOR: STEADY-STATE METABOLIC FLUX VARIATION

M.F.A Bradfield, W. Nicol*

Department of Chemical Engineering, University of Pretoria, Lynnwood Road, Hatfield, 0002, Pretoria, South Africa

Postal address: Department of Chemical Engineering, University of Pretoria,

Private Bag X20, Hatfield, 0028, South Africa

E-mail addresses:

Prof. W. Nicol; corresponding author: willie.nicol@up.ac.za

Mr. M.F.A Bradfield: michael.bradfield@tuks.co.za

*Corresponding author. Tel.: +27 12 420 3796; fax: +27 12 420 5048. E-mail address: willie.nicol@up.ac.za

Abstract

Continuous anaerobic fermentations were performed in a novel external-recycle, biofilm reactor using D-glucose and CO_2 as carbon substrates. Succinic acid (SA) yields were found to be an increasing function of glucose consumption with the succinic acid to acetic acid ratio increasing from 2.4 g g^{-1} at a glucose consumption of 10 g L^{-1}, to 5.7 g g^{-1} at a glucose consumption of 50 g L^{-1}. The formic acid to acetic acid ratio decreased from an equimolar value (0.77 g g^{-1}) at a glucose consumption of 10 g L^{-1} to a value close to zero at 50 g L^{-1}. The highest SA yield on glucose and highest SA titre obtained were 0.91 g g^{-1} and 48.5 g L^{-1} respectively. Metabolic flux analysis based on the established C_3 and C_4 metabolic pathways of *Actinobacillus succinogenes* revealed that the increase in the succinate to acetate ratio could not be attributed to the decrease in formic acid and that an additional source of NADH was present. The fraction of unaccounted NADH increased with glucose consumption, suggesting that additional reducing power is present in the medium or is provided by the activation of an alternative metabolic pathway.

Keywords

Fermentation, biofilms, bioreactors, succinic acid, metabolic flux analysis.

1. Introduction

Succinic acid (SA) or butanedioic acid has various important applications in the pharmaceutical, food, biopolymers and chemicals industry [1] and has been identified as a potential large-scale, biomass-derived chemical by the US Department of Energy [2,3]. SA is conventionally produced from crude oil-based precursors via an expensive, complex process with potential environmental costs [4]. With this in mind and the expected growth in the market for SA, present developments in SA production focus on a biological process based on the conversion of a renewable feedstock to SA by a biocatalyst. Biological SA production assimilates carbon dioxide (a possible environmental benefit) and is not directly dependent on crude oil. Presently, the most favourable biocatalysts for SA production are wild strains of *Actinobacillus succinogenes* [5], *Mannheimia succiniciproducens* [6], *Anaerobiospirillum succiniciproducens* [7] and recombinant strains of *Escherichia coli* [8], with *A. succinogenes* showing promise due to its ability to naturally produce SA at a high titre [1] and its high acid tolerance [9].

Metabolic flux analysis can be used to assess the productivity and limitations of a biocatalyst under different operating conditions as well as to identify and examine the influence of alternative pathways on flux distribution [10]. The performance of a bioreactor is closely linked to flux distribution as it has a strong influence on yield, titre and production rate; important parameters in the economic viability of a process [11]. The central metabolic network of *A. succinogenes* (Fig.1) consists of a C_3 and C_4 pathway [12]. Succinate is formed in the C_4 pathway via phosphoenolpyruvate carboxykinase and the reductive branch of the TCA cycle. Acetate and formate are formed in the C_3 pathway where pyruvate can be converted via two pathways, the pyruvate dehydrogenase pathway or the pyruvate formate-lyase pathway.

Current studies on SA production in batch and continuous reactors reflect that *A.succinogenes* is a competitive SA producer [13–18]. These studies report obtained yields and by-product distributions but do not attempt to reconcile the results with the central metabolic network by analysing the metabolic flux distribution. Variations in product distributions are reported in these studies although the redox implications of the variations are not explored. Van Heerden and Nicol [19] performed a partial metabolic analysis where it was shown that all continuous results exclusively follow the pyruvate formate-lyase route.

Constant product distributions were obtained at all the dilution rates but no redox checks were performed.

Steady-state metabolic flux distribution can be best assessed in a continuous fermentation at steady-state since the constant environmental conditions (i.e. no perturbations) should ensure that metabolic flux distribution remains fixed. Moreover, continuous operation is essential if bio-production of SA is to achieve production rates and quantities competitive with conventional production techniques, as the biocatalyst cost per mass of product can be significantly reduced in a continuous system [20]. Therefore, it is important to understand the behaviour of the biocatalyst and the variations in its metabolic flux distribution in a continuous fermentation. To date, no studies have been performed on the metabolic flux distribution of *A.succinogenes* in a continuous reactor under steady-state conditions. This work presents important insights into the limits of the metabolic flux distribution of *A.succinogenes* in a continuous biofilm reactor.

2. Materials and Methods

2.1. Microorganism

A. succinogenes 130Z (DSM 22257 or ATCC 55618) was acquired from the German Collection of Microorganisms and Cell Cultures (DSMZ). Vials containing treated beads in a cryopreservation solution were used to store culture samples at -75 °C. Inoculum was incubated at 37 °C and 100 rpm for 16 – 24 hours in 30 mL sealed vials containing 15 mL sterilised tryptone soy broth (TSB).

2.2. Growth medium

All chemicals were obtained from Merck KgaA (Darmstadt, Germany), unless otherwise indicated. The fermentation medium consisted of three parts: a growth medium, a phosphate buffer and glucose. The growth medium, based on Urbance et al. [21], had the following composition: 6.0 g L^{-1} yeast extract, 10.0 g L^{-1} clarified corn steep liquor (Sigma-Aldrich, St. Louis, USA), 1.0 g L^{-1} NaCl, 0.2 g L^{-1} $MgCl_2 \cdot 6H_2O$, 0.2 g L^{-1} $CaCl_2 \cdot 2H_2O$, 1.36 g L^{-1} sodium acetate, 2.5 – 5 mL Antifoam A (Sigma-Aldrich. St. Louis, USA) and 0.16 g L^{-1} $Na_2S \cdot 9H_2O$ (for anaerobic conditions). Corn steep liquor was clarified by boiling a 200 g L^{-1} solution at 105 °C for 15 min and allowing the solids to precipitate during cooling. Once cooled, the supernatant was removed and used for the growth medium. The phosphate buffer consisted of 3.2 g L^{-1} KH_2PO_4 and 1.6 g L^{-1} K_2HPO_4. The D-glucose concentration varied from 30 g L^{-1} to 60 g L^{-1}. A glucose concentration of 30 g L^{-1} was used primarily during the start-up phase of each fermentation, thereafter the concentration was increased. CO_2(g) (Afrox, Johannesburg, South Africa) was fed into the recycle line at between 3% and 10% vvm to serve as the inorganic carbon source.

2.3. Fermentation

The novel bioreactor, illustrated in Fig. 2, consisted of a glass cylinder contained between an aluminium base and head, connected by an external recycle for agitation. The total open (void) volume of the reactor (including the recycle) was 158 mL. The glass body of the reactor was incompletely filled to provide a head space which assisted in foam control. All gas inlets and outlets, including reservoir vents, contained 0.2 µm PTFE membrane filters (Midisart 2000, Sartorius, Göttingen, Germany). Gas vented from the reactor via an outlet on the reactor head and passed through a foam-trap which prevented foam blockage of the filter. A thermocouple was housed within an aluminium sheath and connected in-line within the

recycle stream. Temperature was controlled at 37 °C using a hotplate coupled to the thermocouple. pH was measured using a Tophit CPS471D ISFET probe (Endress+Hauser, Gerlingen, Germany) housed within a stainless-steel holder connected in-line within the recycle stream. pH was controlled at 6.80 using a Liquiline CM442 (Endress+Hauser, Gerlingen, Germany) where an internal relay controlled the dosing of 10 M, unsterilised NaOH in an on-off fashion.

The three parts of the fermentation medium (growth medium, buffer and glucose) were prepared in separate bottles and connected to the reactor system. The entire reactor system (excluding NaOH) was autoclaved at 121 °C for 40 min. To prevent unwanted reactions amongst the medium components, the three medium parts were only mixed once the system had cooled to room temperature. The reactor was filled with medium and once temperature and pH stabilised, 10 mL of inoculum was injected into the reactor through a silicon septum attached to the reactor head. Fermentations were initialised by operating the system at a low dilution rate to allow for cells to accumulate without the possibility of washout. An exit pump was used to control the level of the reactor and compressed air was continuously fed through the exit line to create positive pressure which assists in aseptic sampling. To improve biofilm stability and increase the total biomass concentration in the reactor, stainless-steel wool was used as packing in one fermentation while in the other fermentation biofilm attachment occurred on the glass, tubing and aluminium sections of the reactor. The stainless-steel was loosely placed into the glass portion of the reactor. Additional antifoam was dosed into the reactor when necessary. Results were generated in two fermentations with durations of 950 h and 1300 h after the moment of inoculation. Dilution rate was varied from 0.05 to 0.50 h^{-1}.

2.4. Analytical methods

High-performance liquid chromatography was used to determine the concentrations of glucose, ethanol and organic acids. Analyses were performed using an Agilent 1260 Infinity HPLC (Agilent Technologies, USA), equipped with an RI detector and a 300 mm x 7.8 mm Aminex HPX-87 H ion-exchange column (Bio-Rad Laboratories, USA). The mobile phase (0.3 mL L^{-1} H_2SO_4) flowrate was 0.6 mL min^{-1} and column temperature was 60 °C. Dry cell weight (DCW) was determined from 9 mL samples or 24-h samples (volume of sample dependent on dilution rate) centrifuged at 12100 x g for 1.5 min and 3095 x g for 10 min, respectively. Cell pellets were washed twice with distilled water and centrifuged between washes then dried at 85 °C for at least 24 h.

2.5. Data analysis and collection

Online monitoring of the process was performed in a similar fashion to that of van Heerden and Nicol [19] where the time-averaged NaOH dosing fraction was linked to a productivity factor allowing an estimated SA concentration to be calculated in real-time. When the time-averaged dosing profile ceased to fluctuate over time, it was assumed that the system had reached pseudo steady-state and the product stream was sampled.

Determining DCW proved problematic as clumps of biofilm detached from the main reactor volume as well as the outlet line and entered the sample. Samples with biofilm clumps resulted in DCW readings ranging from 2.0 g L^{-1} to 2.5 g L^{-1}, while clear samples, typically obtained at lower dilution rates, gave readings below 0.6 g L^{-1}. Variations in DCW were addressed towards the end of the study where 24-h steady-state samples allowed for fluctuations to average out.

Overall mass balances were performed to assess the accuracy of each sample. The mass balances were performed by comparing the stoichiometric amount of glucose required to achieve the experimental C_{SA}, C_{AA} and C_{FA} to the experimentally obtained amount of glucose consumed. The percentage closure is calculated as the required stoichiometric amount of glucose divided by the experimental amount of glucose consumed. DCW in the outlet was ignored due to the mentioned fluctuations. The mass balances closed to 94% on average with a standard deviation of 3.5% which suggests that more glucose was consumed than needed to account for metabolite production. The additional glucose is likely used in biomass synthesis as the 24-h samples with low DCWs closed to 97.8% with a standard deviation of 3.3%.

2.6. Dilution rate as independent variable

Biofilm formation was unavoidable from the onset of all fermentations. It was also noted that a specific dilution rate was not associated with a specific consumption of glucose, hinting that the active biomass content in the reactor (X_{tot}) was dependent on the operation history of the fermentation characterised by periods of growth, degradation, disintegration and periods of apparent stability. Steady states remained stable for extended periods (up to seven days) but were not repeatable since control of X_{tot} was not possible due to its dependence on the history of the fermentation. In general higher SA titres and glucose consumptions were obtained at lower dilution rates, although major variations were observed for different steady states at a given dilution rate due to biofilm fluctuations. Since volumetric productivity cannot be

related to dilution rate, X_{tot} should be used as the basis for the bioreactor design equation, where the biomass residence time (X_{tot}/Q) will be the true independent variable. X_{tot} is difficult to determine and requires termination of the fermentation while assumptions with regard to the active fraction of biomass need to be made. The rate function will relate the glucose consumption to X_{tot}/Q where glucose consumption will increase with X_{tot}/Q. Accordingly the glucose consumption was used as a relative indicator of X_{tot}/Q and used as the independent variable in the results reported below.

3. Results and Discussion

3.1. Metabolic flux variation

Succinic acid concentration (C_{SA}) and acetic acid concentration (C_{AA}) increased with increasing glucose consumption, where C_{SA} increased continuously at an increasing rate and C_{AA} increased at a diminishing rate, approaching a constant value at high values of glucose consumed (Fig. 3). Formic acid concentration (C_{FA}) increased up to 20 g L^{-1} glucose consumed and showed a steadily decreasing trend towards zero with increasing glucose consumption. Glucose concentrations in the outlet varied between 5 g L^{-1} and 41 g L^{-1} with no substrate limitation occurring (Fig. 3). Ethanol concentrations were found to be negligible. In the event of constant metabolic flux across all values of glucose consumed, the acid concentrations should all increase linearly. Since Fig. 3 indicates that the acid concentrations did not follow a linear profile, the steady-state metabolic flux of *A. succinogenes* varied with increasing glucose consumption. Furthermore, it is evident that the flux shifted in favour of SA production at increasing values of glucose consumed. A trend line was fitted to C_{SA} in Fig. 3, accentuating the non-linear relationship between the outlet SA concentration and glucose consumed (ΔGL). The fit had an R^2 value of 0.98 which reflects the consistency of the increasing trend of C_{SA} as a function of glucose consumed despite the data being generated in two independent fermentations.

Metabolic flux distribution is best represented by the ratios (or relative yields) of the metabolites resulting from different metabolic pathways. Metabolite ratios are independent of the overall mass balance closure when biomass flux is negligible. These ratios therefore provide a more accurate indication of the metabolite distribution than overall yields (e.g. Y_{GLSA}) which are directly dependent on the accuracy of the mass balances. As such, the flux distribution of *A. succinogenes* can be represented by the succinic acid to acetic acid (Y_{AASA}), and the formic acid to acetic acid (Y_{AAFA}) ratios. The yield of SA on glucose (Y_{GLSA}) serves as an additional flux distribution parameter but is more prone to exhibit experimental error than metabolite ratios due to imperfect mass balance closures. The shift in metabolic flux mentioned above is therefore further evidenced by variations in the metabolite ratios as illustrated in Fig. 4, where Y_{AASA} increased and Y_{AAFA} decreased with increasing glucose consumption. The appreciable increase in Y_{AASA} exemplifies the flux shifting in favour of SA production.

3.2. Theoretical analysis of metabolic flux distribution

Optimising carbon flux to SA is essential for the bio-production of SA to be commercially competitive. Wild-type *A.succinogenes* produces SA via the phosphoenolpyruvate (PEP) carboxykinase pathway and the reductive branch of the TCA cycle (C_4 pathway, Fig. 1). There is a net consumption of NADH along this route and therefore, in the absence of excess NADH, acetic acid and formic acid are produced via pyruvate conversion (C_3 pathway) to complete the metabolism of carbon and satisfy the redox balance. Flux to SA is therefore constrained owing to the need to satisfy the redox balance. The metabolism of pyruvate by *A. succinogenes* can occur via two pathways, namely the pyruvate formate-lyase pathway (PFL) or the pyruvate dehydrogenase pathway (PDH). In the PFL route, Y_{AAFA} is 1.0 mol mol^{-1} since the acetyl-CoA formed from pyruvate is converted into a single AA molecule (Fig. 1). Alternatively, if the PDH pathway is active, no FA is produced but instead CO_2 and NADH, hence Y_{AAFA} is zero and additional reducing power is generated. Similarly, if the PFL pathway is active in conjunction with formate dehydrogenase (FDH), CO_2 and NADH are produced in the breakdown of FA by FDH resulting in Y_{AAFA} becoming zero. The following reactions occur when pyruvate is converted exclusively by PFL:

$$\mathrm{GL} + 2\mathrm{CO_2} + 2\mathrm{NADH} \rightarrow 2\mathrm{SA} \quad (1)$$

$$\mathrm{GL} \rightarrow 2\mathrm{AA} + 2\mathrm{FA} + 2\mathrm{NADH} \quad (2)$$

Equation (1) represents SA production while equation (2) represents AA and FA production. Combining (1) and (2) yields the net, redox balance equation (3):

$$\mathrm{GL} + \mathrm{CO_2} \rightarrow \mathrm{SA} + \mathrm{AA} + \mathrm{FA} \quad (3)$$

Equation 3 reflects that the maximum value for Y_{AASA} is 1.0 mol mol^{-1} = 1.97 g g^{-1} and the maximum Y_{GLSA} is 0.66 g g^{-1}, in the event that no biomass is formed, i.e. all carbon is converted to metabolites. Alternatively, if the conversion of pyruvate occurs via PDH the following reactions occur:

$$2\mathrm{GL} + 4\mathrm{CO_2} + 4\mathrm{NADH} \rightarrow 4\mathrm{SA} \quad (4)$$

$$\mathrm{GL} \rightarrow 2\mathrm{AA} + 2\mathrm{CO_2} + 4\mathrm{NADH} \quad (5)$$

Equation (4) is simply equation (1) multiplied by two to satisfy overall redox requirements and equation (5) represents AA production. Similar to above, combining (4) and (5) yields the net, redox balanced equation (6):

$$3GL + 4CO_2 \rightarrow 4SA + 2AA \quad (6)$$

It follows from (6) that, in the absence of biomass formation, the maximum value for Y_{AASA} is 2.0 mol mol^{-1} = 3.93 g g^{-1} and the maximum Y_{GLSA} is 0.87 g g^{-1}. If formic acid is produced via PFL, it is possible for it to be converted to CO_2 and NADH by FDH, which also gives a maximum value of 3.93 g g^{-1} for Y_{AASA}, with no biomass formation. If biomass is synthesised, a portion of glucose will be channelled to anabolic pathways and the redox balance will be affected resulting in maximum yields less than those given above. The above maxima are based on the central metabolism of *A. succinogenes* and pertain specifically to the pathways depicted in Fig. 1.

Despite the limitations given above, Y_{AASA} in this study consistently increased above values of 3.93 g g^{-1} at glucose consumptions greater than 30 g L^{-1} (Fig. 4), showing an upward trend to a maximum value of 5.70 g g^{-1} which indicates a shift in metabolic flux distribution. Although there is scatter of the data in Fig. 4, the shift in metabolic flux distribution is evident since *all* the measured Y_{AASA} values of this study clearly exceed the theoretical maxima and do so to an increasing extent with increasing glucose consumption.

The highest Y_{AASA} values for batch fermentations on glucose with *A. succinogenes* found in literature are 15.33 g g^{-1} [22] with minimal growth medium; 8.92 g g^{-1} [23] with corn steep liquor and heme; 5.60 g g^{-1} [14] with yeast extract and corn steep liquor; and 5.20 g g^{-1} [13] with yeast extract. However, in continuous fermentations the highest Y_{AASA} values achieved were only 2.77 g g^{-1} [17] and 2.5 g g^{-1} [19]. This study therefore achieved the highest Y_{AASA} in continuous fermentations with *A. succinogenes* to date but the batch results from literature suggest that *A. succinogenes* may be capable of achieving greater Y_{AASA} values in a continuous fermentation. Note that other fermentation studies on *A. succinogenes* do not report all metabolite concentrations or product yields and therefore metabolic flux distributions cannot be assessed in these cases.

Furthermore, Y_{AAFA} decreased towards zero with increasing glucose consumption, suggesting an increase in either PDH or FDH activity. The lowest Y_{AAFA} values found in literature for batch fermentations are 0 g g^{-1} [22], 0.61 g g^{-1} [23], 0.69 g g^{-1} [14] and 0.81 g g^{-1} [13]. In continuous fermentations Kim et al. [17] achieved the lowest Y_{AAFA} value of 0.81 g g^{-1} whereas van Heerden and Nicol [19] reported equimolar amounts of FA and AA. Therefore, this study is the first to report a decrease of Y_{AAFA} to zero in a continuous fermentation with *A. succinogenes*. The redox balance dictates an increase in Y_{AASA} following a decrease in

Y_{AAFA} as described by the solid black line in Fig. 4. The linear fit to the experimental Y_{AAFA} data given in Fig. 4 was used to generate the solid black line depicting predicted Y_{AASA} values. It is interesting to note that the experimental Y_{AASA} values exceeded the predicted values. This implies that an increase in PDH or FDH activity is not the only contribution to the increase in Y_{AASA} and that an alternative source of reducing power is present.

The highest Y_{GLSA} achieved in this study was 0.91 g g^{-1} with the yields exceeding 0.68 g g^{-1} under all conditions. The maximum observed Y_{GLSA} exceeds the theoretical limit of 0.87 g g^{-1}. The highest Y_{GLSA} values reported for continuous fermentations with *A. succinogenes* are 0.76 g g^{-1} [18], 0.69 g g^{-1} [19] and 0.59 g g^{-1} [17], and the highest achieved in a batch fermentation is 0.94 g g^{-1} [14]. Therefore this study achieved the highest Y_{GLSA} in a continuous fermentation with *A. succinogenes* to date and similarly to the discussion on Y_{AASA} above, the batch studies on *A. succinogenes* suggest that higher Y_{GLSA} values may be obtainable in continuous fermentations.

Biomass formation is associated with the net formation of NADPH/NADH and this may account for the redox imbalance. It is useful to analyse the additional or 'excess' NADH required to satisfy the redox balance at high Y_{AASA} as a function of glucose consumption. The 'excess' NADH can be expressed as the moles of NADH generated beyond the pathway in Fig. 1 per mole of glucose consumed (i.e. mol mol^{-1}). The 24-hour sample at a glucose consumption of 41.4 g L^{-1} resulted in a DCW of 0.18 g L^{-1}. Assuming the standard molecular composition of biomass ($CH_{1.8}O_{0.5}N_{0.2}$, [24]) and the metabolic pathway of Fig. 1, the NADH formed via the generation of biomass (0.003 mol mol^{-1}), glycolysis (2.0 mol mol^{-1}) and the PDH/FDH pathway (0.214 mol mol^{-1}) is only 87% of that required (2.543 mol mol^{-1}) to produce 34.5 g L^{-1} SA. The 'excess' NADH is therefore 0.326 mol mol^{-1}. Similar results were obtained for the other 24-hour samples. This implies that the additional reducing power generated from biomass production and the PDH/FDH pathway collectively do not account for the extra NADH required to satisfy the high Y_{AASA} values.

It is also viable to postulate that the growth medium contains an unknown source of reducing power. To explore this possibility the yield profiles given in Fig. 4 were fitted with empirical least squares fits which were used to determine the 'excess' NADH as a function of glucose consumption (Fig. 5) based on metabolic network analysis. It is evident that the additional reducing power increases as the glucose consumption (or X_{tot}/Q) increases. If the potential additional NADH ('free NADH') in the feed was stoichiometrically limited and fully

consumed, higher glucose consumptions would have resulted in a smaller amount of 'free NADH' per glucose consumed. However, the reverse is evident from Fig. 5. It is also plausible that the consumption of 'free NADH' in the medium is rate limited. In such a case, the lower glucose depletion rates at higher glucose consumptions will result in a larger fraction of 'free NADH' per glucose consumed as observed in Fig. 5. Therefore, the medium serving as the source of the additional NADH remains a possibility.

Another possible explanation is that a metabolic process delivers the 'excess' NADH or NADPH. The oxidative branch of the TCA cycle and the glyoxylate shunt are able to independently generate additional NADH thereby increasing C_4 pathway flux and the maximum Y_{GLSA} to 1.12 g g^{-1} without by-product formation, as discussed in van Heerden and Nicol [25]. However, *A. succinogenes* lacks the TCA cycle enzymes citrate synthase and isocitrate dehydrogenase [26] as well as a functional glyoxylate shunt [12] and therefore these pathways can be ruled out as the sources of the additional NADH. Rühl et al. [27] demonstrated that resting, non-growing *Bacillus subtilis* cells show sustained metabolic activity without cell growth which leads to an apparent catabolic NADPH overproduction (via the pentose phosphate pathway) that is converted to NADH by transhydrogenase. A similar mechanism could occur in *A. succinogenes* as it does possess transhydrogenase [12], although it is suggested that the transhydrogenase converts excess NADH to NADPH [28]. If the oxidative pentose phosphate pathway (PPP) is active and carbon is channelled into the pathway via glucose-6-phosphate, and any fructose-6-phosphate produced in the pathway is completely recycled through the pathway [24], the following net reactions can occur:

$$3\mathrm{GL} \rightarrow 2\mathrm{CO_2} + 8\mathrm{NADH} + 4\mathrm{SA} \quad (7)$$

$$\frac{1}{2}\mathrm{GL} + \mathrm{CO_2} + \mathrm{NADH} \rightarrow \mathrm{SA} \quad (8)$$

Equation 7 represents the overall oxidative pathway leading to SA via the PPP. The equation is based on the assumption that any glyceraldehyde-3-phosphate that forms in the PPP is converted to PEP with the release of one NADH, and that PEP is subsequently channelled to SA via the C_4 pathway. Furthermore, it is assumed that the NADPH produced in the oxidative PPP is converted to NADH by transhydrogenase. Equation 8 reflects the overall reductive pathway when SA is produced from glucose via the reverse TCA cycle. When Equations 7 and 8 are combined and the redox is balanced, the following net reaction results:

$$7\mathrm{GL} + 6\mathrm{CO_2} \rightarrow 12\mathrm{SA} \quad (9)$$

From Equation 9 it is evident that if no biomass or by-products are formed the maximum yield of SA on glucose (Y_{GLSA}) is 1.12 g g^{-1} which is equivalent to the effect of a complete TCA cycle or glyoxylate shunt as mentioned above. Therefore, increased yields of SA on glucose and greater SA-to-by-products ratios can be achieved with an active oxidative PPP as it delivers sufficient reducing power eliminating the need for C_3 pathway flux. Such a mechanism could explain the source of the additional reducing power observed in this study.

It is known that cell growth is inhibited by the organic acids produced by *A.succinogenes* [9,13,18,29]. Despite the growth inhibition due to high acid concentrations, the results from batch fermentations with *A.succinogenes* suggest that organic acids continue to be produced after cell growth termination [9,13,15,22,23] which tends to occur between 11 g L^{-1} and 28 g L^{-1} total acids concentration and 8 g L^{-1} and 19 g L^{-1} succinate concentration, depending on the medium and fermentation conditions. This suggests that *A.succinogenes* is capable of producing SA, AA and FA in a non-growth or maintenance state. Furthermore, in certain batch fermentations with *A. succinogenes* [13,15,22,23], the data suggest that the metabolic flux distribution shifted in favour of SA production at the point where cell growth terminated. The shift is reflected by an increase in Y_{AASA} as the biomass concentration decreased. In the present study, an average DCW of 0.19 g L^{-1} was obtained from three 24-h samples, where an established biofilm was present and the system was in pseudo-steady state. Y_{AASA} during the sampling intervals was between 3.8 g g^{-1} and 4.5 g g^{-1} with glucose consumption between 40 g L^{-1} and 44 g L^{-1}. On the contrary, DCWs in situations with less observed biofilm were greater (1.7 g L^{-1} to 2.4 g L^{-1}) and Y_{AASA} was between 2.6 g g^{-1} and 3.5 g g^{-1} with glucose consumption between 19 g L^{-1} and 27 g L^{-1}. Although the absolute values of the DCWs are questionable (as discussed in section 2.5), the differences in magnitude qualitatively suggest a difference in the behaviour of the bacteria. At high SA concentrations the growth of biomass appears to decrease (i.e. decrease in DCW in the fermenter outlet) which could imply the cells have entered a maintenance or non-growth state as mentioned above. Furthermore, the accompanied increase in Y_{AASA} suggests that succinate production is favoured in this state. The notion of *A. succinogenes* entering a maintenance state with a different metabolic flux distribution ties in with the work by Rühl et al. [27], and it is possible that the additional reducing power is generated by sustained activity of the pentose phosphate pathway. However, this suggestion is speculative at best and an investigation into whether the pentose phosphate pathway is active will be required. The presence of biofilm may play a role in enhancing the variation in metabolic flux as biofilm can comprise cells expressing distinct

metabolic pathways [30] and the maintenance state may therefore be more pronounced in sessile cells. Also, the higher Y_{AASA} values were obtained with an established biofilm.

As mentioned above, Y_{AAFA} was found to decrease from 0.77 g g^{-1} (equimolar amounts) to values approaching zero (Fig. 4). Furthermore, Y_{AASA} tended to be greater than 1.97 g g^{-1} for all amounts of glucose consumed which suggests that either the PDH pathway or the FDH pathway (after initial FA production via PFL), or both, is active and becomes increasingly so with increasing glucose consumption. Van der Werf et al. [31] determined the specific activity of PDH, PFL and FDH in end product formation in *A. succinogenes* to be: less-than-1, 390 and 12 nmol min^{-1} mg $protein^{-1}$ respectively. Moreover, in batch experiments with *A. succinogenes* Xi et al. [22] and Du et al. [16] report that C_{FA} increased up to a point then decreased as the fermentation proceeded. The higher FDH activity and decrease in C_{FA} with time in some batch fermentations provides evidence that the PFL-FDH pathway is likely the primary route of pyruvate metabolism.

4. Conclusions

This study provides evidence that the metabolic flux distribution of *A. succinogenes* in a continuous biofilm reactor is a function of glucose consumption. More specifically, C_{SA} increased continuously with increasing glucose consumption while the concentrations of the other metabolites, acetate and formate, flattened out and decreased to zero, respectively. Furthermore, succinic acid production (i.e. flux to the C_4 metabolic pathway) was favoured at high values of glucose consumption, when the cells are probably in a maintenance or non-growth state and therefore express different metabolic pathways, allowing greater yields. Values greater than the theoretical maximum values were obtained for Y_{AASA} (5.70 g g^{-1}) and Y_{GLSA} (0.91 g g^{-1}). In addition, Y_{AAFA} was consistently less than 0.77 g g^{-1} and approached zero as C_{FA} decreased, which suggests that either the PDH or the FDH pathway, or a combination thereof, becomes increasingly active with increasing glucose consumption. These pathways, and biomass synthesis, allow for an increase in Y_{AASA} due to NADH generation, but could not account for the total increase, which is probably explainable by the activation of alternative metabolic pathways that generate additional NADH or by the presence of additional reducing power in the medium.

Nomenclature

ΔGL glucose consumed (g L^{-1})

AA acetic acid

C concentration (g L^{-1})

DCW dry cell weight

FA formic acid

FDH formate dehydrogenase

GL glucose

PDH pyruvate dehydrogenase

PEP phosphoenolpyruvate

PFL pyruvate formate-lyase

PPP pentose phosphate pathway

Q volumetric flow rate (mL min^{-1})

SA succinic acid

Y_{ij} yield of species j on species i (g_j g_i^{-1})

X_{tot} total active biomass amount (g)

Acknowledgements

The financial assistance of the National Research Foundation (NRF) towards this research is hereby acknowledged.

References

[1] J.G. Zeikus, M.K. Jain, P. Elankovan, Biotechnology of succinic acid production and markets for derived industrial products, Appl. Microbiol. Biotechnol. 51 (1999) 545–552.

[2] T. Werpy, G. Petersen, Top value added chemicals from biomass, Volume 1. Results of screening for potential candidates from sugars and synthesis gas, 2004.

[3] J.J. Bozell, G.R. Petersen, Technology development for the production of biobased products from biorefinery carbohydrates—the US Department of Energy's "Top 10" revisited, Green Chem. 12 (2010) 539.

[4] H. Song, S.Y. Lee, Production of succinic acid by bacterial fermentation, Enzyme Microb. Technol. 39 (2006) 352–361.

[5] M. Guettler, D. Rumler, M. Jain, Actinobacillus succinogenes sp. nov., a novel succinic-acid-producing strain from the bovine rumen, Int. J. Syst. Bacteriol. 49 (1999) 207–216.

[6] I. Oh, H. Lee, C. Park, S.Y. Lee, J. Lee, Succinic acid production by continuous fermentation process using Mannheimia succiniciproducens LPK7, J. Microbiol. Biotechnol. 18 (2008) 908–912.

[7] P.C. Lee, W.G. Lee, S. Kwon, S.Y. Lee, H.N. Chang, Batch and continuous cultivation of Anaerobiospirillum succiniciproducens for the production of succinic acid from whey, Appl. Microbiol. Biotechnol. 54 (2000) 23–7.

[8] H. Lin, G.N. Bennett, K.-Y. San, Fed-batch culture of a metabolically engineered Escherichia coli strain designed for high-level succinate production and yield under aerobic conditions, Biotechnol. Bioeng. 90 (2005) 775–9.

[9] S.K.C. Lin, C. Du, A. Koutinas, R. Wang, C. Webb, Substrate and product inhibition kinetics in succinic acid production by Actinobacillus succinogenes, Biochem. Eng. J. 41 (2008) 128–135.

[10] J. Nielsen, Metabolic engineering: techniques for analysis of targets for genetic manipulations, Biotechnol. Bioeng. 58 (1998) 125–32.

[11] J.J. Beauprez, M. De Mey, W.K. Soetaert, Microbial succinic acid production: Natural versus metabolic engineered producers, Process Biochem. 45 (2010) 1103–1114.

[12] J.B. McKinlay, Y. Shachar-Hill, J.G. Zeikus, C. Vieille, Determining Actinobacillus succinogenes metabolic pathways and fluxes by NMR and GC-MS analyses of 13C-labeled metabolic product isotopomers, Metab. Eng. 9 (2007) 177–92.

[13] R.I. Corona-González, A. Bories, V. González-Álvarez, C. Pelayo-Ortiz, Kinetic study of succinic acid production by Actinobacillus succinogenes ZT-130, Process Biochem. 43 (2008) 1047–1053.

[14] M. Guettler, M. Jain, D. Rumler, Method for making succinic acid, bacterial variants for use in the process, and methods for obatining variants, U.S. Patent 5,573,931, 1996.

[15] Y.-P. Liu, P. Zheng, Z.-H. Sun, Y. Ni, J.-J. Dong, L.-L. Zhu, Economical succinic acid production from cane molasses by Actinobacillus succinogenes, Bioresour. Technol. 99 (2008) 1736–42.

[16] C. Du, S.K.C. Lin, A. Koutinas, R. Wang, P. Dorado, C. Webb, A wheat biorefining strategy based on solid-state fermentation for fermentative production of succinic acid, Bioresour. Technol. 99 (2008) 8310–5.

[17] M. Il Kim, N.-J. Kim, L. Shang, Y.K. Chang, S.Y. Lee, H.N. Chang, Continuous Production of Succinic Acid Using an External Membrane Cell Recycle System, J. Microbiol. Biotechnol. 19 (2009) 1369–1373.

[18] S.E. Urbance, A.L. Pometto, A. a Dispirito, Y. Denli, Evaluation of succinic acid continuous and repeat-batch biofilm fermentation by Actinobacillus succinogenes using plastic composite support bioreactors, Appl. Microbiol. Biotechnol. 65 (2004) 664–70.

[19] C.D. van Heerden, W. Nicol, Continuous succinic acid fermentation by Actinobacillus succinogenes, Biochem. Eng. J. 73 (2013) 5–11.

[20] J. Wöltinger, A. Karau, W. Leuchtenberger, K. Drauz, Membrane Reactors at Degussa, Adv Biochem Engin/Biotechnol. 92 (2005) 289–316.

[21] S.E. Urbance, A.L. Pometto, A. a. DiSpirito, A. Demirci, Medium Evaluation and Plastic Composite Support Ingredient Selection for Biofilm Formation and Succinic Acid Production by Actinobacillus succinogenes, Food Biotechnol. 17 (2003) 53–65.

[22] Y. Xi, K. Chen, R. Xu, J. Zhang, X. Bai, M. Jiang, et al., Effect of biotin and a similar compound on succinic acid fermentation by Actinobacillus succinogenes in a chemically defined medium, Biochem. Eng. J. 69 (2012) 87–92.

[23] Y. Xi, K. Chen, W. Dai, J. Ma, M. Zhang, M. Jiang, et al., Succinic acid production by Actinobacillus succinogenes NJ113 using corn steep liquor powder as nitrogen source, Bioresour. Technol. 136 (2013) 775–9.

[24] J. Villadsen, J. Nielsen, G. Lidén, Bioreaction Engineering Principles, Third, Springer US, Boston, MA, 2011.

[25] C.D. van Heerden, W. Nicol, Continuous and batch cultures of Escherichia coli KJ134 for succinic acid fermentation: metabolic flux distributions and production characteristics., Microb. Cell Fact. 12 (2013) 80.

[26] J.B. McKinlay, J.G. Zeikus, C. Vieille, Insights into Actinobacillus succinogenes fermentative metabolism in a chemically defined growth medium, Appl. Environ. Microbiol. 71 (2005) 6651–6.

[27] M. Rühl, D. Le Coq, S. Aymerich, U. Sauer, 13C-flux analysis reveals NADPH-balancing transhydrogenation cycles in stationary phase of nitrogen-starving Bacillus subtilis, J. Biol. Chem. 287 (2012) 27959–70.

[28] J.B. McKinlay, C. Vieille, 13C-metabolic flux analysis of Actinobacillus succinogenes fermentative metabolism at different NaHCO3 and H2 concentrations, Metab. Eng. 10 (2008) 55–68.

[29] R.I. Corona-Gonzalez, A. Bories, V. González-Alvarez, R. Snell-Castro, G. Toriz-González, C. Pelayo-Ortiz, Succinic acid production with Actinobacillus succinogenes ZT-130 in the presence of succinic acid, Curr. Microbiol. 60 (2010) 71–7.

[30] P.S. Stewart, M.J. Franklin, Physiological heterogeneity in biofilms, Nat. Rev. Microbiol. 6 (2008) 199–210.

[31] M.J. van der Werf, M. V Guettler, M.K. Jain, J.G. Zeikus, Environmental and physiological factors affecting the succinate product ratio during carbohydrate fermentation by Actinobacillus sp. 130Z, Arch. Microbiol. 167 (1997) 332–42.

Figure captions

Fig. 1. Simplified metabolic network of *A. succinogenes* showing the pathways leading to its major metabolites (based on McKinlay et al. [12]). The relevant enzymes are (1) pyruvate formate lyase (PFL), (2) pyruvate dehydrogenase (PDH), and (3) formate dehydrogenase (FDH).

Fig. 2. Simplified schematic of the bioreactor setup (not to scale).

Fig. 3 Metabolic flux distribution represented as acid concentrations for a given amount of glucose consumed. The open markers represent data from van Heerden [19]. Each datum represents a sample of the bioreactor at pseudo-steady state.

Fig. 4 The maximum Y_{AASA} for a given pathway is shown by the broken lines at 3.93 g g^{-1} and 1.97 g g^{-1}. The solid line between the two Y_{AASA} maxima represents the maximum Y_{AASA} based on the corresponding Y_{AAFA} value (determined from the trendline through the data points and a carbon and redox balance). The open markers are selected data from van Heerden [19].

Fig. 5 Excess NADH required to produce the corresponding SA at a given glucose consumption relative to NADH generated by the central metabolic network of *A. succinogenes*.

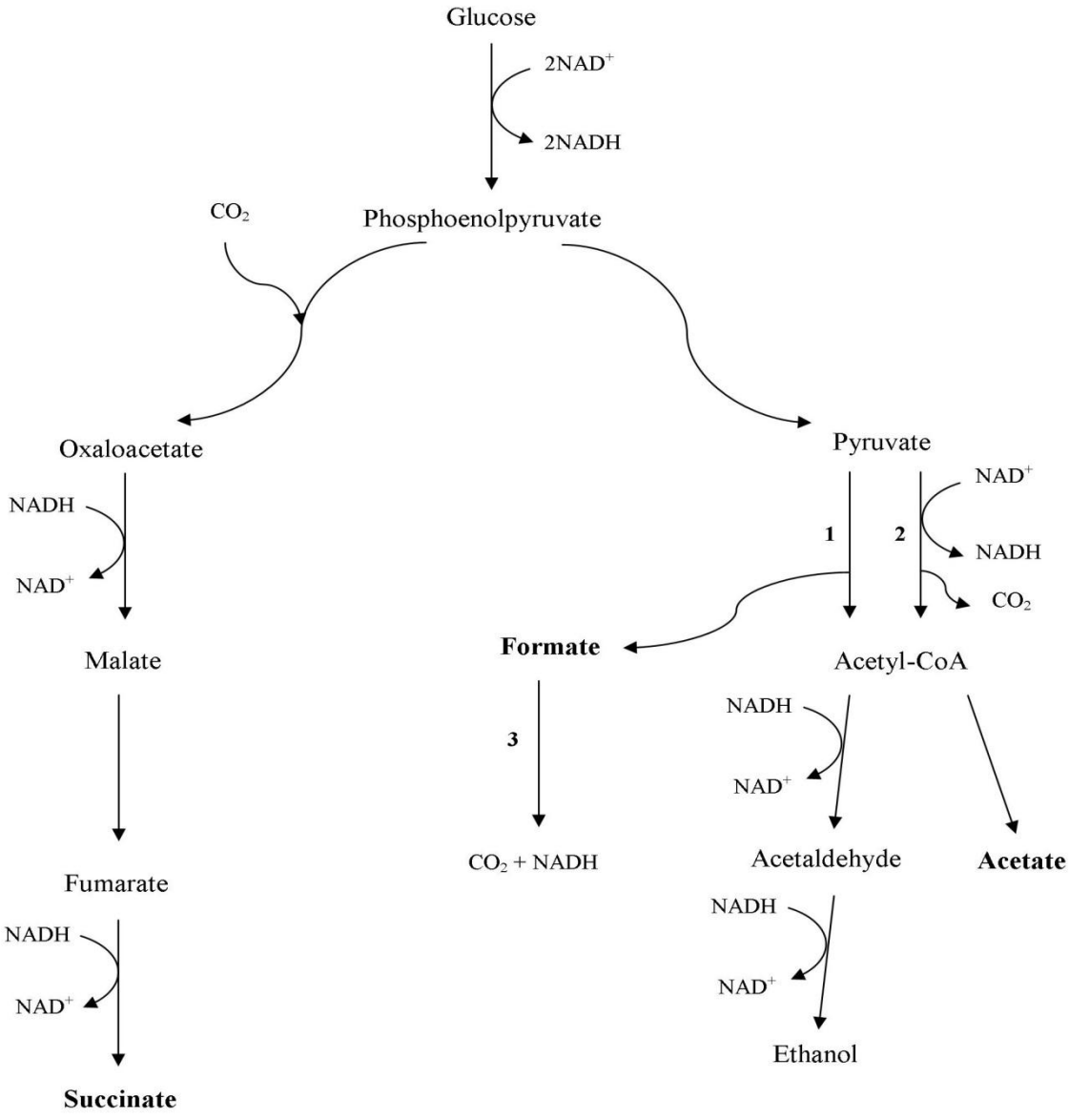

Fig. 1 Simplified metabolic network of *A. succinogenes* showing the pathways leading to its major metabolites (based on McKinlay et al. [12]). The relevant enzymes are (1) pyruvate formate-lyase, (2) pyruvate dehydrogenase and (3) formate dehydrogenase.

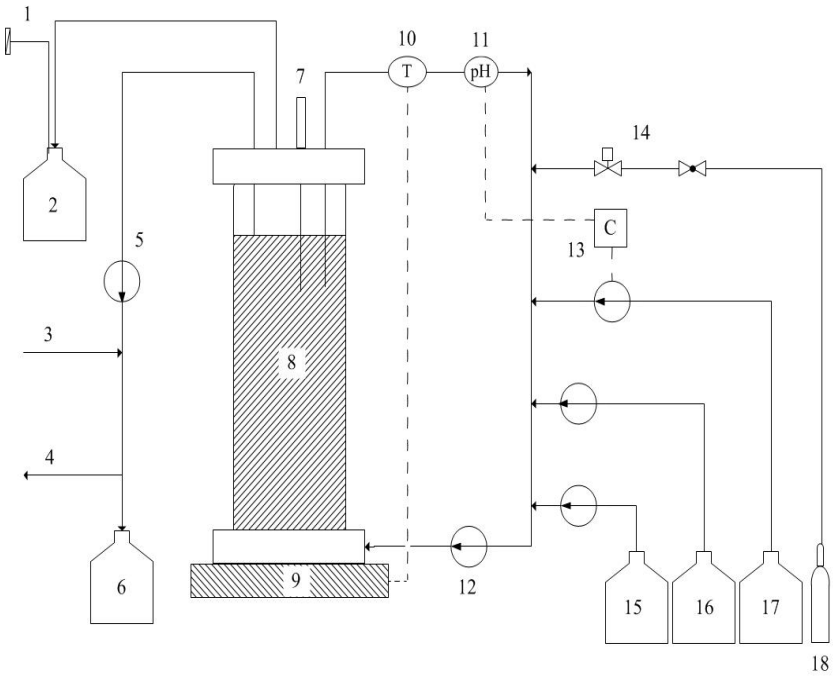

No.	Description
1	Gas filter
2	Foam-trap
3	Compressed air purge
4	Sample line
5	Peristaltic pump
6	Product reservoir
7	Inoculation septum
8	Reactor body
9	Hot plate
10	Thermocouple & temp. controller
11	pH probe
12	Recycle pump
13	pH controller
14	Gas flow controller
15	Medium reservoir
16	Antifoam reservoir
17	NaOH reservoir
18	CO_2 cylinder

Fig. 2 Simplified schematic of the bioreactor setup (not to scale).

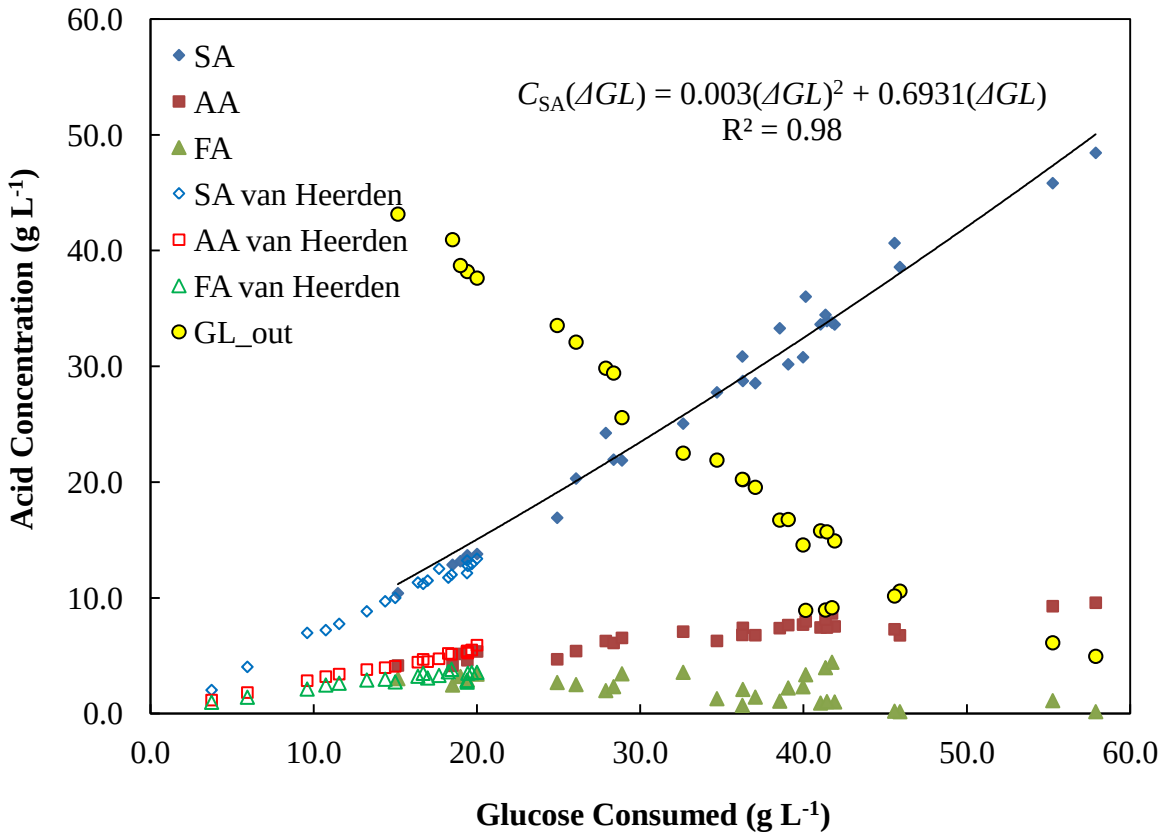

Fig. 3 Metabolic flux distribution represented as acid concentrations for a given amount of glucose consumed. The open markers represent data from van Heerden [19]. Each datum represents a sample of the bioreactor at pseudo-steady state.

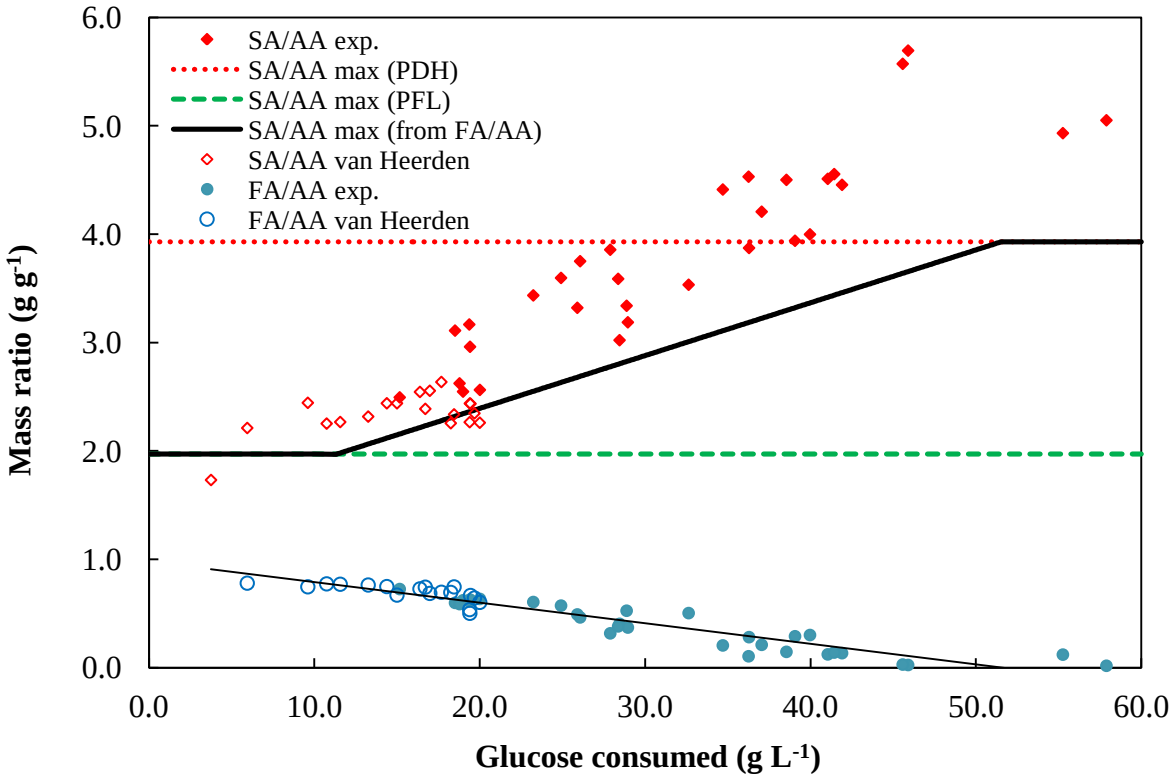

Fig. 4 The maximum Y_{AASA} for a given pathway is shown by the broken lines at 3.93 g g^{-1} and 1.97 g g^{-1}. The solid line between the two Y_{AASA} maxima represents the maximum Y_{AASA} based on the corresponding Y_{AAFA} value (determined from the trendline through the data points and a carbon and redox balance). The open markers are selected data from van Heerden [19].

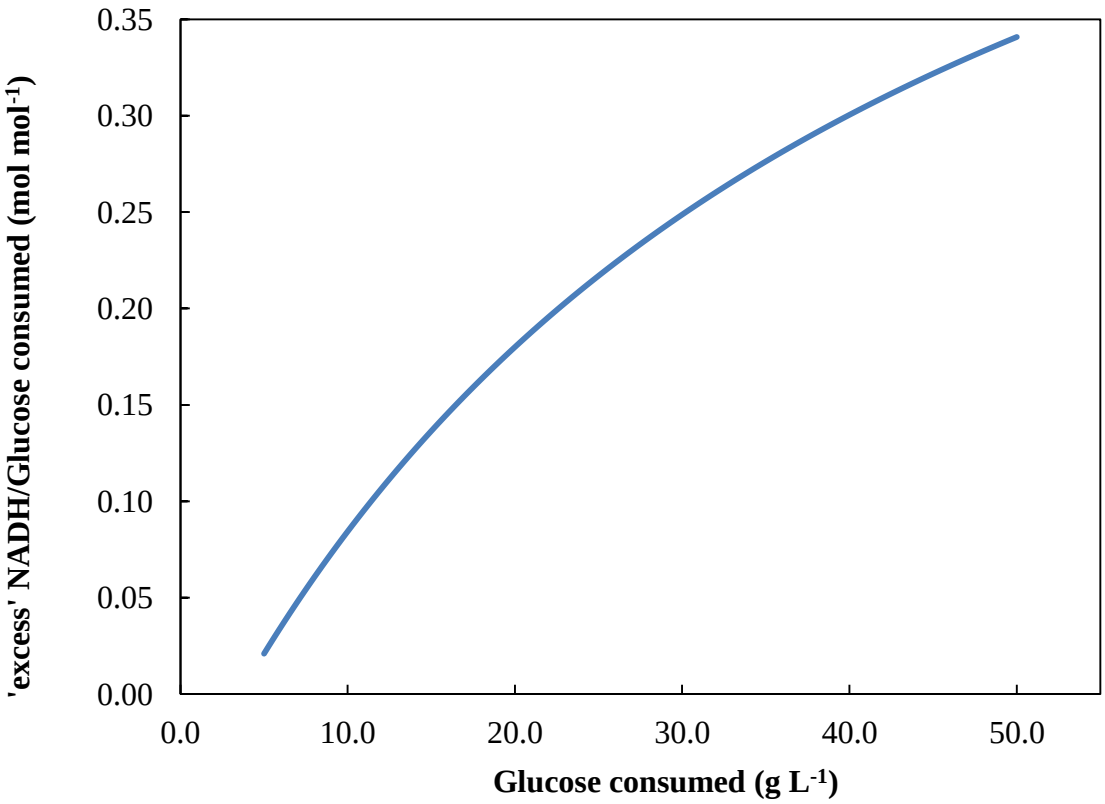

Fig. 5 Excess NADH required to produce the corresponding SA at a given glucose consumption relative to NADH generated by the central metabolic network of *A. succinogenes*.

Highlights

- Metabolic flux to succinic acid favoured at high succinic acid titres
- Formic acid production decreased to zero at high glucose consumption
- Redox closure shows additional NADH source when considering accepted metabolic map